

Lipschitz-Based Robustness Certification Under Floating-Point Execution

TOBY MURRAY, University of Melbourne, Australia

Sensitivity-based robustness certification has emerged as a practical approach for certifying neural network robustness, including in settings that require verifiable guarantees. A key advantage of these methods is that certification is performed by concrete numerical computation (rather than symbolic reasoning) and scales efficiently with network size. However, as with the vast majority of prior work on robustness certification and verification, the soundness of these methods is typically proved with respect to a semantic model that assumes exact real arithmetic. In reality deployed neural network implementations execute using floating-point arithmetic. This mismatch creates a semantic gap between certified robustness properties and the behaviour of the executed system.

As motivating evidence, we exhibit concrete counterexamples showing that real arithmetic robustness guarantees can fail under floating-point execution, even for previously verified certifiers, with discrepancies becoming pronounced at lower-precision formats such as float16. We then develop a formal, compositional theory relating real arithmetic Lipschitz-based sensitivity bounds to the sensitivity of floating-point execution under standard rounding-error models, specialised to feed-forward neural networks with ReLU activations. We derive sound conditions for robustness under floating-point execution, including bounds on certificate degradation and sufficient conditions for the absence of overflow. We formalize the theory and its main soundness results, and implement an executable certifier based on these principles, which we empirically evaluate to demonstrate its practicality.

1 Introduction

Robustness is an important property for helping to ensure the trustworthiness of neural network classifier outputs. Given a neural network N produces output class $\text{ArgMax}(N(x))$ for input x , we say that this answer is *robust* if the neural network would have outputted the same class for any nearby input x' within distance ε of x : $\forall x'. \|x - x'\| \leq \varepsilon \implies \text{ArgMax}(N(x')) = \text{ArgMax}(N(x))$.

A range of robustness-checking techniques have been developed. These include techniques that *verify* the robustness of neural network outputs using symbolic reasoning, for example via abstract interpretation over relational domains [39] or specialised solvers [20]. A closely related class of approaches applies abstract interpretation over lightweight numeric abstract domains, such as zonotope- and interval-based methods [38], in order to improve verification scalability at the expense of precision.

A third class of approaches *certify* robustness via sensitivity analysis, by performing concrete numerical computation (rather than maintaining symbolic constraints or abstract program states) such as computing Lipschitz or norm-based sensitivity bounds [30, 46]. These methods therefore typically enjoy better scalability-precision tradeoffs. Recent work has further shown how the implementations of such certification procedures themselves can be formally verified [42].

Most existing approaches to robustness certification and verification (except for a few robustness verifiers and abstract interpreters—see e.g. [38–40, 52]), assume the neural network executes with real arithmetic semantics. Deployed neural network implementations instead operate via floating-point arithmetic. This creates a semantic gap between the arithmetic semantics assumed by the verifier or certification procedure and the deployed execution semantics—a discrepancy that has recently been highlighted as a central programming languages challenge in neural network verification [7]. Prior work has shown that this gap can give rise to concrete robustness *counterexamples* that robustness verifiers will verify as robust [19], despite the existence of nearby inputs that the neural network classifies differently.

We investigate this gap in the context of sensitivity-based robustness certification, where it has received less attention despite the aforementioned benefits of this class of robustness checking approaches, and show how to address it while preserving the benefits of certification. We focus specifically on Lipschitz-based (global) robustness certification (Section 2.1) for neural networks executing under standard floating-point semantics (Section 2.2). We begin (Section 2.3) by showing that the conservatism of this certification method does not on its own rule out the possibility of producing misleading certifications, by exhibiting concrete robustness counter-examples that are nonetheless certified by methods that assume neural network execution conforms to real arithmetic.

While our theory is general, we specialise it to feed-forward neural networks employing ReLU activations on all hidden layers, and the identity activation on the output layer (Section 3.1). We reason about floating-point arithmetic under the standard model (Section 3.2) of round-to-nearest with gradual underflow [17].

This model holds only in the absence of overflow. Therefore, we first (Section 4) derive sufficient conditions to check the absence of overflow in neural network computations. We then (Section 5) develop a compositional theory for reasoning about the deviation between real and floating-point arithmetic in these computations, in the absence of overflow. We employ this theory to show (Section 6) how classical real arithmetic Lipschitz-based robustness certification checks [30] can be adapted to account for floating-point execution, including the degree to which robustness margins are degraded by this accounting. We also show how (Section 7), for the use case of certifying robustness for a model pre-deployment over its test set, we can significantly reduce this degradation by employing a *hybrid* certification method that takes measurements from high-precision (e.g., float64) model executions.

We implement our approach and empirically evaluate its performance (Section 8) over recent benchmarks for Lipschitz-based robustness certification [42], including MNIST and CIFAR-10 globally-robust trained [30] networks. We show how floating-point accounting rules out the possibility of producing the kinds of misleading certifications (Section 2.3) we use to motivate our work. We also investigate the degree to which floating-point accounting degrades robustness certificates in practice, finding that robustness certification remains practical. Finally, we compare our pre-deployment hybrid certification method to the ERAN robustness verifier [35], showing that it generally achieves a comparable degree of precision while being many orders of magnitude more efficient.

We formalise all of our results in the Rocq theorem [5] (version 8.20.1) prover on top of the LAMProof library [23], which is a formalisation of the standard error models [17] for reasoning about floating-point arithmetic linear algebra operations.

Use of generative AI. This research and the resulting paper were produced using Generative AI serving in much the same role as a research student under the author’s supervision (albeit without the benefit of any learning taking place except by the author). The key ideas that this paper embodies were developed in conversation between the author and ChatGPT. Theorems and proofs were first developed in conversation with ChatGPT, iterating in a generate-then-manual-audit loop producing highly-detailed proofs (approx. 23 pages) that the author manually audited for correctness. Those results were then formalised in Rocq using Claude Code, over several weeks, producing Rocq theories that total approx. 9,000 source lines of code. The author carefully audited the key definitions and top-level theorem statements, to ensure that the pen-and-paper mathematics was faithfully captured. Many, many rounds of auditing and iteration were required to produce faithful encodings. The only axioms employed by the Rocq proofs are an axiomatisation of the key properties of matrix spectral norms.

The author implemented the certification procedures described in this paper in Python using Claude Code. The resulting code comprises a real arithmetic certification kernel which validates its own outputs against those of the formally verified certifier of Tobler et al. [42]. Remaining functionality was carefully audited to check its conformance with the Rocq formalisation and its presentation in this paper. Parts of the counter-example search procedure described in Section 2.3 were developed with ChatGPT.

The author takes full responsibility for any errors due to the use of generative AI in conducting the research reported in this paper. Generative AI (Claude Code and ChatGPT) were used during the drafting of this manuscript; however, its final contents is the sole responsibility of the author.

2 Background and Motivation

2.1 Robustness and Lipschitz-Based Certification

We can view a neural network as a function N from inputs x to outputs y , where x and y are vectors of some fixed dimensions respectively. We focus exclusively on neural network classifiers, which classify inputs x into $|y|$ output classes, where $|y|$ is the length of output vectors y . Specifically, given an output y , y 's output class is given by the index of its maximum component: $\text{ArgMax}(y)$.

In this paper we focus on l_2 robustness: given a perturbation bound ε , output $y = N(x)$ produced from input x is robust for ε whenever N classifies all inputs x' within ε of x identically to x , where distance is measured via the Euclidean norm (written $\|v\|_2$ for vector v).

Definition 2.1. Given $\varepsilon > 0$ and input x , which produces output $y = N(x)$, we say that x (equivalently y) is *robust* iff:

$$\forall x'. \|x - x'\|_2 \leq \varepsilon \implies \text{ArgMax}(N(x')) = \text{ArgMax}(y).$$

We write $B(x, \varepsilon) := \{x' \mid \|x - x'\|_2 \leq \varepsilon\}$ for the closed ε -ball centred at x ; robustness of x is then the condition that N classifies every $x' \in B(x, \varepsilon)$ identically to x .

Fix an input x and its associated output $y = N(x)$. Let $i^* = \text{ArgMax}(y)$ denote the output class of x , and let j be any other *competing* class. We write $m_{j,i^*}(x)$ to denote the *margin* between the output and competing class at input x , which is simply $y_{i^*} - y_j$. This definition generalises to arbitrary inputs x' : $m_{j,i^*}(x') = N(x')_{i^*} - N(x')_j$. Robustness of x is enforced whenever this margin remains positive for all x' within ε of x , i.e., whenever for each competitor class $j \neq i^*$ we have

$$\forall x'. \|x - x'\|_2 \leq \varepsilon \implies m_{j,i^*}(x') > 0.$$

While many certified robustness techniques exist, a prominent class of methods involves computing quantities that bound the sensitivity of the neural network's output to changes in its input. One such instance first proposed by Leino et al. [30] involves checking margin positivity for each $j \neq i^*$ by computing for each j a margin Lipschitz constant L_{j,i^*} , which bounds the degree to which the margin $m_{j,i^*}(\cdot)$ changes per change in the model's input:

$$\forall x_1, x_2. \frac{|m_{j,i^*}(x_1) - m_{j,i^*}(x_2)|}{\|x_1 - x_2\|_2} \leq L_{j,i^*}.$$

Methods for computing margin Lipschitz constants are outside the scope of this paper, but include iterative approximation algorithms, whether from below as in power iteration [15], or from above as in Gram iteration [8]. With margin Lipschitz constants computed, certifying robustness for an input x requires simply checking for each $j \neq i^*$ that

$$m_{j,i^*}(x) > L_{j,i^*} \cdot \varepsilon.$$

2.2 Real vs. Floating-Point Arithmetic

The discussion above was purposefully vague about the types of the components of x , y , and so on. In fact, the soundness of Lipschitz-based margin certification assumes that all numeric types and arithmetic are real numbers. This applies both to the certification implementation as well as to the neural network implementation that is being certified.

Tobler et al. [42] provide a verified implementation for computing Lipschitz constants and performing the certification checks using arbitrary precision rational numbers, i.e., without loss of precision. However, as they note, the quantities that their implementation computes are sound only under the assumption that the neural network operates using real arithmetic. In practice, however, neural network implementations operate using floating-point arithmetic, which serves as an efficient, fixed-precision approximation of real arithmetic.

This raises the question of whether this discrepancy—between the real arithmetic assumed for the soundness of Lipschitz-based margin certification, and the reality of floating-point arithmetic in deployed neural networks—can give rise to situations in which the quantities computed by a sound robustness certifier (particularly the margin Lipschitz constants) do not accurately describe the behaviour of the neural network being certified. If this were to happen, might such a sound certifier be able to return misleading answers? Specifically, claiming that an input x is robust (because it would be under real arithmetic) when in reality the model might yield conflicting answers for some x' within ϵ of x ?

2.3 Verified Certified Robustness Counterexamples

Prior work has shown that the discrepancy between floating-point and real arithmetic can cause *complete* robustness verifiers to yield exactly these kinds of misleading answers [19, 54]. A complete robustness verifier is one that, when given an input point x and perturbation bound ϵ such that x is not robust, is able to return sufficient evidence about why x was not robust to allow the construction of a nearby point x' within ϵ of x that is classified differently to x . Prior work [19] has shown how the ability to produce such x' allows one to search for an input x_0 that the verifier claims is robust for ϵ and x_0 is almost exactly ϵ away from the model’s decision boundary such that it is possible to find an adversarial point x_1 that is within ϵ of x_0 but that is classified differently to x_0 . In other words, x_1 is a *counterexample* to the verifier’s claim that x_0 is robust at ϵ .

One way to think about a complete verifier is that its analysis is tight, in the sense that it doesn’t under-estimate robustness. In contrast, sensitivity-based robustness certifiers are typically not complete. In order to be sound and efficient, these kinds of certifiers tend to over-estimate a neural network’s sensitivity and, therefore, under-estimate robustness. For this reason, it is not obvious that such certifiers should also be prone to giving misleading answers due to the discrepancy between floating-point and real arithmetic. For instance, because certification uses *global* margin Lipschitz constants, it upper bounds (and thus over-estimates) the model’s sensitivity for any particular input point x . Perhaps the conservatism introduced by this over-estimation is sufficient to account for floating-point discrepancies.

We investigated this question in the context of Tobler et al.’s formally verified robustness certifier [42]. To do so we developed a straightforward search procedure that given a model identifies triples (x_0, x_1, ϵ) for which x_0 and x_1 are classified differently, $\|x_0 - x_1\|_2 \leq \epsilon$ but x_0 is certified ϵ -robust by Tobler et al.’s verified certifier. In particular, x_1 effectively sits right on the decision boundary and is classified differently to x_0 due to floating-point rounding effects in network execution. The search procedure takes a starting point x_{nat} . From this it finds a nearby point x_t that is classified differently to x_{nat} by applying the DeepFool [34] adversarial search procedure, as implemented in the Adversarial Robustness Toolbox [36] library, version 1.20.1. Linear interpolation

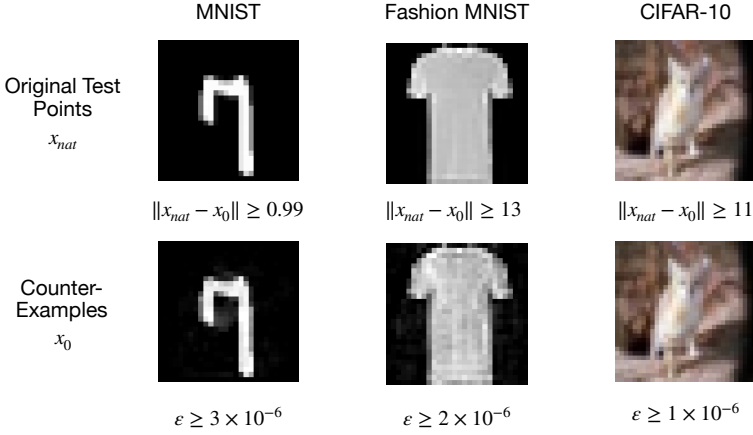


Fig. 1. Instances for which Tobler et al.’s verified certifier produces misleading robustness certifications. x_{nat} is the original test point; x_0 is certified robust at ϵ , yet there exists x_1 within ϵ of x_0 that is classified differently (due to floating-point rounding).

is then applied, with binary search, to find on the line between x_{nat} and x_t an initial pair of points $(x_{0_{init}}, x_1)$ such that $x_{0_{init}}$ is certified robust at $\|x_{0_{init}} - x_1\|_2$ but x_1 lies on the other side of the decision boundary (due to floating-point rounding). This initial $(x_{0_{init}}, x_1)$ is then *expanded* by searching outwards from $x_{0_{init}}$ to find the furthest x_0 that is classified the same as $x_{0_{init}}$ and certified robust at $\epsilon = \|x_0 - x_1\|_2$. The search procedure returns the final (x_0, x_1, ϵ) that it found.

We stress that this search procedure exists merely to find instances that demonstrate how, due to floating-point rounding, sensitivity-based robustness certifiers can give misleading answers—even when formally verified. It is not designed to try to produce instances in which the certified robust point x_0 is necessarily a natural input for the neural network classifier in question, nor for which the found ϵ is necessarily semantically meaningful to the classification problem for which the neural network has been trained.

This search procedure successfully found instances that caused Tobler et al.’s verified certifier to produce misleading answers against the three MNIST [29], Fashion MNIST [49] and CIFAR-10 [27] models respectively against which Tobler et al.’s certifier was originally evaluated [42]. These models utilise float32 arithmetic. Fig. 1 depicts representative instances for each model. The starting points x_{nat} are drawn from the models’ test sets. We show the resulting point x_0 , as well as its distance from the original x_{nat} , and the value of ϵ . Each x_0 is certified robust by Tobler et al.’s verified implementation at its corresponding ϵ ; however, there exists a nearby x_1 (not shown) within ϵ of x_0 that is classified differently to x_0 . We note that each ϵ is incredibly small and well below what is semantically meaningful for each input domain.

We also ran the same search procedure against these models, executed at different levels of floating-point precision: bfloat16, float16, and float64. Fig. 2 shows some representative instances found for the MNIST model. We see that at lower precision it becomes easier to discover instances with larger ϵ that becomes semantically meaningful. This is to be expected because the magnitude of floating-point rounding effects is much larger for low-precision formats like bfloat16 and float16. Floating-point effects are still discernible even at float64, while being very much smaller. The same trends were apparent for the Fashion MNIST and CIFAR-10 models.

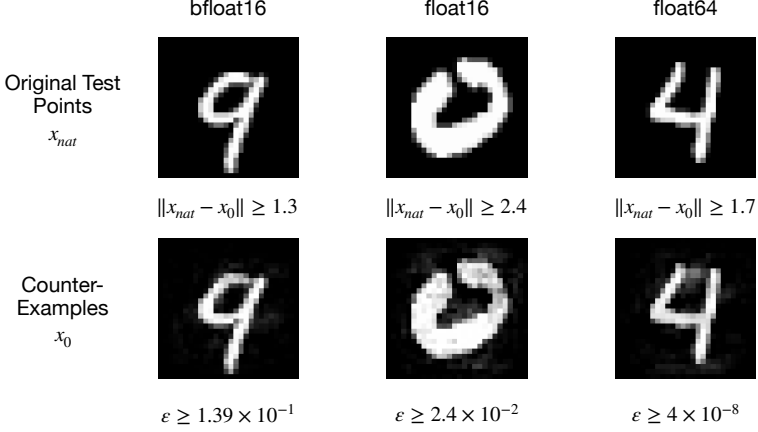


Fig. 2. MNIST instances for which Tobler et al.’s verified certifier produces misleading robustness certifications at various floating-point formats. x_{nat} is the original test point; x_0 is certified robust at ε , yet there exists x_1 within ε of x_0 that is classified differently.

We conclude that certifier conservatism alone does not eliminate the semantic gap between real arithmetic certification and floating-point execution. This motivates the need for a formal account of this gap and how we can address it.

3 Floating-Point Semantics and Deviation from Real Arithmetic

The misleading instances in Section 2.3 arise from discrepancies between real arithmetic reasoning and floating-point execution. In this section, we formalise that discrepancy for dense (i.e., fully-connected) feed-forward neural networks.

3.1 Feed-Forward Neural Networks

We begin by briefly recapping the standard model of these networks, over real arithmetic. Such networks are composed of L layers. Let $\ell \in \{1, \dots, L\}$ be a layer index. Then each layer ℓ comprises a weight matrix $W_\ell \in \mathbb{R}^{m_\ell \times n_\ell}$, bias vector $b_\ell \in \mathbb{R}^{m_\ell}$, and activation function φ_ℓ . Let $x \in \mathbb{R}^{n_1}$ denote the neural network input and $z_{\ell-1}(x)$ denote the input to layer ℓ that is produced when x is fed into the network. Then $z_0(x) = x$. Let a_ℓ denote the layer- ℓ preactivation, defined as

$$a_\ell = W_\ell z_{\ell-1} + b_\ell$$

to which the layer- ℓ activation function is applied to produce the layer- ℓ output:

$$z_\ell = \varphi_\ell(a_\ell).$$

We make the following assumptions on activation functions throughout:

- (i) *Pointwise scalar maps*: each φ_ℓ is a scalar function applied elementwise.
- (ii) *Zero-preserving*: $\varphi_\ell(0) = 0$.
- (iii) *Lipschitz continuous*: φ_ℓ has Lipschitz constant $L(\varphi_\ell) \geq 0$.

- (iv) *FP-exact*: the floating-point evaluation of φ_ℓ agrees with its real arithmetic counterpart for all finite inputs.

As stated in Section 1, we focus on networks with ReLU activations in hidden layers (with $L(\varphi_\ell) = 1$) and identity activation at the output layer ($\varphi_L(z) = z$). Both satisfy all four assumptions. However, assumption (iv) excludes smooth activations such as sigmoid and tanh, whose floating-point implementations introduce rounding; however, our assumptions are satisfied by other comparison-based activations (e.g., absolute value, hard tanh), but such functions are uncommon in practice. Extending the theory to soundly account for activation-function rounding is left to future work.

3.2 Floating-Point Error

We adopt the standard model of floating-point error [17], in which floating-point operations are modelled in terms of their real arithmetic counterparts. This model is applicable to error analysis of standard floating-point formats including IEEE-754 formats like float16, float32 and float64, as well as formats like bfloat16. It is also the model formalised by LAPProof [23], on which our Rocq formalisation rests. Our use of LAPProof assumes round-to-nearest, ties-to-even with gradual underflow, which is the default in floating-point implementations.

This model assumes the existence of positive constants: u , the *unit roundoff*, used to capture the size of the *relative* roundoff error in floating-point operations; a_{mul} is the *absolute* roundoff error for operations like multiplication and division when their result is subnormal. We write $\text{fl}(\cdot)$ to denote the floating-point counterpart of a real valued computation.

Basic operations. The following error model applies to basic operations \circ , when their result does not overflow:

$$\text{fl}(x \circ y) = (x \circ y)(1 + \delta) + \eta, \quad |\delta| \leq u, \quad |\eta| \leq a_{\text{mul}} \quad (1)$$

where δ and η are *input-dependent* terms that account respectively for the relative and absolute error. For addition and subtraction, η is 0. Since a result is either subnormal or not, we also have $\delta \cdot \eta = 0$.

We write F_{max} for the largest finite value representable in the floating-point format; a result *overflows* when its magnitude exceeds F_{max} .

Matrix-vector product and bias addition. From this model of basic operations, one can derive similar models for more complex operations like matrix-vector multiplication of matrix $W \in \mathbb{R}^{m \times n}$ and vector $z \in \mathbb{R}^n$:

$$\text{fl}(Wz) = (W + \Delta W)z + \eta_{\text{mv}}, \quad |\Delta W| \leq \gamma_n |W|, \quad \gamma_n := (1 + u)^n - 1 \leq \frac{nu}{1 - nu}. \quad (2)$$

The vector $\eta_{\text{mv}} \in \mathbb{R}^m$ captures the accumulation of the per-product absolute terms across each length- n dot product. A safe, input-independent bound is

$$|\eta_{\text{mv}}| \leq a_{\text{dot}}(n) \mathbb{1}, \quad a_{\text{dot}}(n) := (1 + \gamma_n) n a_{\text{mul}},$$

interpreted entrywise (here $\mathbb{1}$ is the all-ones vector in \mathbb{R}^m). Passing to the ℓ_2 norm, since each $|\eta_{\text{mv}_i}| \leq a_{\text{dot}}(n)$:

$$\|\eta_{\text{mv}}\|_2 \leq a_{\text{dot}}(n) \sqrt{m}.$$

For bias addition $\text{fl}(v + b)$ of preactivation v and bias $b \in \mathbb{R}^m$, since $\eta = 0$ in (1) for addition, the error is purely relative and entrywise bounded:

$$\text{fl}(v + b) = v + b + \delta_{\text{add}}, \quad |\delta_{\text{add}}| \leq u (|v| + |b|). \quad (3)$$

Squaring, summing over components, and applying Cauchy–Schwarz to the cross term gives

$$\|\delta_{\text{add}}\|_2 \leq u (\|v\|_2 + \|b\|_2).$$

Floating-point network execution and deviation. We define the *floating-point evaluation* of the network by replacing each arithmetic operation with its floating-point counterpart. Given floating-point activations $\hat{z}_{\ell-1}$ from the previous layer, with $\hat{z}_0 = x$, the floating-point preactivation and activation at layer ℓ are:

$$\begin{aligned}\hat{a}_\ell &:= \text{fl}(\text{fl}(W_\ell \hat{z}_{\ell-1}) + b_\ell), \\ \hat{z}_\ell &:= \varphi_\ell(\hat{a}_\ell).\end{aligned}$$

Only the linear operations—the matrix-vector product and bias addition—are subject to floating-point error; assumption (iv) from Section 3.1 ensures the activation step introduces no additional rounding error.

The *floating-point deviation* d_ℓ at layer ℓ is the difference between the floating-point and exact (real arithmetic) activations:

$$d_\ell := \hat{z}_\ell - z_\ell. \quad (4)$$

Our goal later in Section 5 will be to bound $\|d_\ell\|_2$ at each layer ℓ , quantifying the semantic gap between real arithmetic and floating-point network execution.

4 Sound Conditions for Absence of Overflow

The mixed-error model for floating-point operations (1),(2), and (3) applies only in the absence of overflow. Therefore, before bounding the floating-point deviation (Section 5), we must first certify the absence of overflow. We write $z_\ell(x')$ and $\hat{z}_\ell(x')$ for the exact (real arithmetic) and FP activations at layer ℓ produced by input x' , and likewise for other quantities like d_ℓ , etc.

Given an input x , our goal is to certify overflow-freedom not just for x but uniformly for every $x' \in B(x, \varepsilon)$. This requires bounding how large the FP activations can be across the entire perturbation ball. We achieve this using just two layer-by-layer scalar quantities, both computable from the network weights and format parameters alone:

- A *radius* $r_{\ell-1}$: a bound on the real activation norm $\|z_{\ell-1}(x')\|_2$, valid simultaneously for all $x' \in B(x, \varepsilon)$. These radii satisfy a simple recurrence driven by the network’s Lipschitz constants and spectral norms, derived below.
- A *deviation bound* $D_{\ell-1}$: a bound on the accumulated FP error $\|d_{\ell-1}(x')\|_2 = \|\hat{z}_{\ell-1}(x') - z_{\ell-1}(x')\|_2$, valid uniformly for all $x' \in B(x, \varepsilon)$. The derivation of these bounds is the subject of Section 5.

The overflow check at layer ℓ must bound the norm of the FP activation $\hat{z}_{\ell-1}(x')$, since that is what is actually fed into the computation. The radius $r_{\ell-1}$ alone is insufficient for this: the FP activation may differ from the real activation by up to $D_{\ell-1}$. By the triangle inequality,

$$\|\hat{z}_{\ell-1}(x')\|_2 \leq \|z_{\ell-1}(x')\|_2 + \|d_{\ell-1}(x')\|_2 \leq r_{\ell-1} + D_{\ell-1},$$

giving a uniform bound on the FP activation norm across all of $B(x, \varepsilon)$. For the base case $\ell = 1$, the network input is exact ($\hat{z}_0 = z_0 = x$), so $D_0 = 0$ and the bound reduces to $r_0 = \|x\|_2 + \varepsilon$.

The overflow-freedom analysis proceeds in three steps: computing the *deterministic radii* $r_{\ell-1}$ that bound the real activations; applying norm bounds row-by-row, using $r_{\ell-1} + D_{\ell-1}$ as the effective FP activation radius, to obtain per-row quantities $S_{\ell,i}$ and $M_{\ell,i}$; and using a forward error theorem to derive checkable overflow conditions certifying the finiteness of the layer- ℓ FP preactivation. In practice, overflow-checking and deviation-bounding are interleaved layer by layer: the deviation bound $D_{\ell-1}$ from Section 5 feeds into the overflow check at layer ℓ , and the overflow guarantee at layer ℓ in turn enables the deviation bound D_ℓ .

Deterministic radii. We propagate an upper bound r_ℓ on $\|z_\ell(x')\|_2$ that holds for all $x' \in B(x, \varepsilon)$ simultaneously. These *deterministic radii* are defined inductively by

$$\begin{aligned} r_0 &:= \|x\|_2 + \varepsilon, \\ r_\ell &:= L(\varphi_\ell)(\|W_\ell\|_2 r_{\ell-1} + \|b_\ell\|_2), \end{aligned}$$

where $\|W_\ell\|_2$ denotes the spectral norm of W_ℓ . The bound $\|z_\ell(x')\|_2 \leq r_\ell$ holds by induction: the triangle inequality bounds the preactivation norm by $\|W_\ell\|_2 \|z_{\ell-1}\|_2 + \|b_\ell\|_2$, and the Lipschitz assumption on φ_ℓ yields the result.

Row-wise overflow quantities. To certify that $\text{fl}(W_\ell \hat{z}_{\ell-1})$ does not overflow, each output entry is checked individually. Entry i is the dot product $w_{\ell,i} \cdot \hat{z}_{\ell-1}$, where $w_{\ell,i} \in \mathbb{R}^{n_\ell}$ denotes the i -th row of W_ℓ . The following lemma (Theorem 4.1) bounds $|\text{fl}(w_{\ell,i} \cdot \hat{z}_{\ell-1})|$ in terms of the sum of absolute products $\sum_j |w_{\ell,i,j}| |\hat{z}_{\ell-1,j}|$, since FP rounding errors accumulate proportionally to the magnitudes of individual products regardless of sign. By Cauchy–Schwarz, this sum is bounded by:

$$\sum_j |w_{\ell,i,j}| |\hat{z}_{\ell-1,j}| \leq \|w_{\ell,i}\|_2 \cdot \|\hat{z}_{\ell-1}\|_2 \leq \|w_{\ell,i}\|_2 \cdot (r_{\ell-1} + D_{\ell-1}) =: S_{\ell,i}.$$

A bound on the largest individual product, needed to ensure no single multiplication overflows, is given by the ℓ_∞ norm:

$$\max_j |w_{\ell,i,j}| |\hat{z}_{\ell-1,j}| \leq \|w_{\ell,i}\|_\infty \cdot (r_{\ell-1} + D_{\ell-1}) =: M_{\ell,i}.$$

Both $S_{\ell,i}$ and $M_{\ell,i}$ are computable from the fixed network weights, $r_{\ell-1}$, and $D_{\ell-1}$.

The following lemma is established in our Rocq formalisation building on LAPProof’s error model [23]. Here $a_{\text{dot}}^{\text{fwd}}(n) := (1 + \gamma_{n-1}) n a_{\text{mul}}$; the use of γ_{n-1} rather than γ_n reflects that a length- n dot product involves n multiplications but only $n - 1$ additions.

LEMMA 4.1 (FORWARD ERROR FOR FP DOT PRODUCTS). *Let a, b be length- n floating-point vectors. If $\sum_j |a_j| |b_j| \leq S$, $|a_j| |b_j| \leq M$ for all j , $M < F_{\text{max}}$, and $S(1 + \gamma_n) + a_{\text{dot}}^{\text{fwd}}(n) < F_{\text{max}}$, then $\text{fl}(a \cdot b)$ is finite and*

$$|\text{fl}(a \cdot b)| \leq S(1 + \gamma_n) + a_{\text{dot}}^{\text{fwd}}(n).$$

Instantiating with $S = S_{\ell,i}$ and $M = M_{\ell,i}$ (with $n = n_\ell$, the input dimension of layer ℓ , i.e., the length of the dot products), the product $\text{fl}(w_{\ell,i} \cdot \hat{z}_{\ell-1})$ is finite whenever

$$M_{\ell,i} < F_{\text{max}} \quad \text{and} \quad S_{\ell,i}(1 + \gamma_{n_\ell}) + a_{\text{dot}}^{\text{fwd}}(n_\ell) < F_{\text{max}},$$

and its magnitude is bounded by $S_{\ell,i}(1 + \gamma_{n_\ell}) + a_{\text{dot}}^{\text{fwd}}(n_\ell)$. To certify that the subsequent bias addition also does not overflow, we check

$$S_{\ell,i}(1 + \gamma_{n_\ell}) + a_{\text{dot}}^{\text{fwd}}(n_\ell) + \|b_\ell\|_\infty < F_{\text{max}},$$

where $\|b_\ell\|_\infty$ is the worst-case bias entry across all rows. No additional rounding factor is needed for the bias addition itself: since the exact sum $|\text{fl}(w_{\ell,i} \cdot \hat{z}_{\ell-1}) + b_{\ell,i}|$ is bounded by $S_{\ell,i}(1 + \gamma_{n_\ell}) + a_{\text{dot}}^{\text{fwd}}(n_\ell) + \|b_\ell\|_\infty < F_{\text{max}}$, and F_{max} is itself a representable floating-point value, round-to-nearest guarantees the computed result is finite.

Layer-wide conditions. The per-row conditions can be reduced to two scalar checks per layer by taking the worst case over all rows. Define

$$\begin{aligned} S_\ell &:= \max_i \|w_{\ell,i}\|_2 \cdot (r_{\ell-1} + D_{\ell-1}), \\ M_\ell &:= \max_i \|w_{\ell,i}\|_\infty \cdot (r_{\ell-1} + D_{\ell-1}). \end{aligned}$$

Since $S_{\ell,i} \leq S_\ell$ and $M_{\ell,i} \leq M_\ell$ for all i , these layer-wide quantities dominate all per-row conditions. Both depend only on the fixed network weights, $r_{\ell-1}$, and $D_{\ell-1}$, making them efficiently checkable.

THEOREM 4.2 (LAYERWISE OVERFLOW-FREEDOM). *Let $\hat{z}_{\ell-1}$ be a finite floating-point vector with $\|\hat{z}_{\ell-1}\|_2 \leq r_{\ell-1} + D_{\ell-1}$, and let W_ℓ, b_ℓ be finite floating-point weights and bias. If $S_\ell(1 + \gamma_{n_\ell}) + a_{\text{dot}}^{\text{fwd}}(n_\ell) + \|b_\ell\|_\infty < F_{\text{max}}$ and $M_\ell < F_{\text{max}}$, then the preactivation $\hat{a}_\ell = \text{fl}(\text{fl}(W_\ell \hat{z}_{\ell-1}) + b_\ell)$ is finite.*

Since assumption (iv) (from Section 3.1) guarantees that φ_ℓ is evaluated exactly, finiteness of the preactivation $\hat{a}_\ell = \text{fl}(\text{fl}(W_\ell \hat{z}_{\ell-1}) + b_\ell)$ immediately implies finiteness of the activation $\hat{z}_\ell = \varphi_\ell(\hat{a}_\ell)$. Thus Theorem 4.2 certifies overflow-freedom for the full layer computation.

Interleaved forward induction. Applying Theorem 4.2 layer by layer – with $D_{\ell-1}$ supplied by Section 5 – reduces overflow certification to two scalar inequalities per layer: the conditions $S_\ell(1 + \gamma_{n_\ell}) + a_{\text{dot}}^{\text{fwd}}(n_\ell) + \|b_\ell\|_\infty < F_{\text{max}}$ and $M_\ell < F_{\text{max}}$ of Theorem 4.2. Together, these constitute a sound certificate of overflow-freedom for the *entire* perturbation ball $B(x, \varepsilon)$.

Practical applicability. While our overflow analysis is sound for all network widths and precisions, the tightness of the bounds depends critically on the product $n_\ell \cdot u$ at each layer. When $n_\ell \cdot u \ll 1$, the error accumulation factor $\gamma_{n_\ell} = (1 + u)^{n_\ell} - 1$ scales approximately linearly with $n_\ell \cdot u$, yielding practical bounds. However, when $n_\ell \cdot u \geq 1$ for any layer, γ_{n_ℓ} exhibits superlinear growth, causing the overflow bounds to become too conservative for practical use. This limits applicability to combinations of network width and precision where $n_\ell \cdot u < 1$ for all layers; we return to this point in Section 8.

5 Bounding Deviation Between Real and Floating-Point Execution

The mixed-error model of Section 3.2 applies only in the absence of overflow. We therefore assume throughout this section that the conditions of Theorem 4.2 hold at each layer, so that every FP operation is finite and the model applies. Our goal is to derive, for each layer $\ell = 1, \dots, L-1$, a computable scalar D_ℓ such that $\|d_\ell(x')\|_2 \leq D_\ell$ simultaneously for all $x' \in B(x, \varepsilon)$. We treat layers up to $L-1$ here because the final layer is handled separately in Section 6: the relevant quantity there is not $\|d_L\|_2$ but the deviation in the output *margins*, which requires a different analysis fed by D_{L-1} .

The bounds D_1, \dots, D_{L-1} satisfy the two-coefficient linear recurrence

$$D_\ell = \alpha_\ell D_{\ell-1} + \beta_\ell(r_{\ell-1}),$$

where the amplification factor α_ℓ and the fresh-error term $\beta_\ell(r)$ depend only on the network weights and format constants.

Setup. Recall from (2) that $\text{fl}(W_\ell \hat{z}_{\ell-1}) = (W_\ell + \Delta W_\ell) \hat{z}_{\ell-1} + \eta_{\text{mv}}$ with $|\Delta W_\ell| \leq \gamma_{n_\ell} |W_\ell|$ entrywise. By the dominated-spectral-norm inequality ($\|A\|_2 \leq \|B\|_2$ whenever $|A_{ij}| \leq B_{ij}$), this gives $\|\Delta W_\ell v\|_2 \leq \gamma_{n_\ell} \| |W_\ell| \|_2 \|v\|_2$ for any vector v , where $\| |W_\ell| \|_2$ is the spectral norm of the entrywise-absolute-value matrix $|W_\ell|$.

The following lemma bounds the one-step deviation $\|d_\ell\|_2$ in terms of the previous-layer deviation $\|d_{\ell-1}\|_2$ and the activation norms $\|z_{\ell-1}\|_2$ and $\|\hat{z}_{\ell-1}\|_2$. Its four-term form is unavoidable: each term corresponds to a distinct source of rounding error in the layer computation. Directly after presenting this lemma we will show how substituting the radius bounds $r_{\ell-1}$ collapses these four terms into the simple two-coefficient recursion $\|d_\ell\|_2 \leq \alpha_\ell \|d_{\ell-1}\|_2 + \beta_\ell(r_{\ell-1})$.

LEMMA 5.1 (ONE-STEP FLOATING-POINT DEVIATION). *Suppose the conditions of Theorem 4.2 hold at layer ℓ . Then, for any $x' \in B(x, \varepsilon)$, with $d_\ell, d_{\ell-1}, z_{\ell-1}$, and $\hat{z}_{\ell-1}$ denoting the respective quantities*

evaluated at input x' ,

$$\begin{aligned} \|d_\ell\|_2 \leq L(\varphi_\ell) & \left[(\|W_\ell\|_2 + \gamma_{n_\ell} \| |W_\ell| \|_2) \|d_{\ell-1}\|_2 \right. \\ & + \gamma_{n_\ell} \| |W_\ell| \|_2 \|z_{\ell-1}\|_2 \\ & + u((1 + \gamma_{n_\ell}) \| |W_\ell| \|_2 \|\hat{z}_{\ell-1}\|_2 + \|b_\ell\|_2) \\ & \left. + (1 + u) a_{\text{dot}}(n_\ell) \sqrt{m_\ell} \right]. \end{aligned} \quad (5)$$

Linear recursion. (5) involves both $\|z_{\ell-1}\|_2$ (the *exact* activation, bounded by the deterministic radius $r_{\ell-1}$ from Section 4) and $\|\hat{z}_{\ell-1}\|_2$ (the *FP* activation). We eliminate both in favour of $r_{\ell-1}$ and $\|d_{\ell-1}\|_2$ by substituting:

$$\|z_{\ell-1}\|_2 \leq r_{\ell-1}, \quad \|\hat{z}_{\ell-1}\|_2 \leq \|z_{\ell-1}\|_2 + \|d_{\ell-1}\|_2 \leq r_{\ell-1} + \|d_{\ell-1}\|_2.$$

Expanding and grouping by coefficient of $\|d_{\ell-1}\|_2$ versus $r_{\ell-1}$, we define

$$\kappa_{n_\ell} := \gamma_{n_\ell} + u(1 + \gamma_{n_\ell}),$$

which combines the relative rounding factor γ_{n_ℓ} from the matrix-vector product with the additional factor $u(1 + \gamma_{n_\ell})$ from the bias-add rounding of the matvec result. Setting

$$\begin{aligned} \alpha_\ell & := L(\varphi_\ell) (\|W_\ell\|_2 + \kappa_{n_\ell} \| |W_\ell| \|_2), \\ \beta_\ell(r) & := L(\varphi_\ell) \left(\kappa_{n_\ell} \| |W_\ell| \|_2 \cdot r + u \|b_\ell\|_2 + (1 + u) a_{\text{dot}}(n_\ell) \sqrt{m_\ell} \right), \end{aligned}$$

we obtain the following.

COROLLARY 5.2 (LINEAR RECURSION FOR DEVIATION). *For every $x' \in B(x, \varepsilon)$ and every layer $\ell \geq 1$,*

$$\|d_\ell(x')\|_2 \leq \alpha_\ell \|d_{\ell-1}(x')\|_2 + \beta_\ell(r_{\ell-1}).$$

The coefficient α_ℓ is the *amplification factor*: for ReLU networks ($L(\varphi_\ell) = 1$) it approximates $\|W_\ell\|_2$, with an FP correction of $\kappa_{n_\ell} \| |W_\ell| \|_2$; and $\beta_\ell(r_{\ell-1})$ captures the *fresh rounding error* at layer ℓ , dominated by $\kappa_{n_\ell} \| |W_\ell| \|_2 r_{\ell-1}$. In practice, for float32 and float64 networks of MNIST or CIFAR-10 scale, both coefficients are only marginally perturbed from the quantities they approximate: α_ℓ is essentially $\|W_\ell\|_2$ and $\beta_\ell(r_{\ell-1}) \ll r_{\ell-1}$. For lower-precision formats such as float16, however, κ_{n_ℓ} can become significantly inflated even for these relatively small networks, causing both α_ℓ and β_ℓ to grow substantially, and the accumulated deviation D_{L-1} to far exceed the perturbation radius, causing the analysis to become vacuous. We return to this point in Section 8.

Cumulative deviation bound. Since the network input is exact ($\hat{z}_0 = z_0 = x$), the base case is $D_0 := 0$. Define

$$D_\ell := \alpha_\ell D_{\ell-1} + \beta_\ell(r_{\ell-1}), \quad \ell = 1, \dots, L-1.$$

A straightforward induction using Theorem 5.2 establishes that $\|d_\ell(x')\|_2 \leq D_\ell$ simultaneously for all $x' \in B(x, \varepsilon)$. The recursion unrolls to the closed form

$$D_\ell = \sum_{j=1}^{\ell} \beta_j(r_{j-1}) \cdot \prod_{i=j+1}^{\ell} \alpha_i,$$

where each summand is the fresh rounding error from layer j , amplified by every subsequent layer. These cumulative bounds D_1, \dots, D_{L-1} are exactly the values $D_{\ell-1}$ consumed by Section 4's overflow check at layer ℓ ; each is available before its layer is processed since it was derived from the previous layer's certificate, so there is no circularity.

The radius bounds (r_ℓ) enter the recursion only through $\beta_\ell(r_{\ell-1})$, so any sequence satisfying $\|z_\ell(x')\|_2 \leq r_\ell$ for all $x' \in B(x, \varepsilon)$ may be used in place of the deterministic radii of Section 4. Input-specific tighter bounds can reduce β_ℓ and yield less conservative deviation estimates; however, in our experience they do so only marginally for significant extra complexity.

6 Robustness Certification under Floating-Point Execution

We now have overflow-freedom (Section 4) and deviation bounds D_1, \dots, D_{L-1} for hidden layers (Section 5). To certify robustness, we must ensure that every output *margin* $m_{j,i^*}(x') = y_{j,i^*}(x') - y_j(x')$ remains positive across $B(x, \varepsilon)$ for all competing classes $j \neq i^*$, where $i^* = \text{ArgMax}(N(x))$ is the predicted class at x . Under floating-point execution, margins become $\hat{m}_{j,i^*}(x') = \hat{y}_{j,i^*}(x') - \hat{y}_j(x')$. The challenge is that $\|d_L\|_2$ bounds the *vector* deviation at layer L , but does not directly tell us how much each individual margin *component* deviates. Our goal is to derive computable conditions that guarantee floating-point margins stay positive.

Final-layer pairwise deviation. We need to bound $|\hat{m}_{j,i^*}(x') - m_{j,i^*}(x')|$, the floating-point deviation in a single margin. At layer L , the network computes $\hat{y} = W_L \hat{z}_{L-1} + b_L$ (followed by identity activation), where $\hat{z}_{L-1}(x')$ is the floating-point activation from layer $L-1$ with deviation bound D_{L-1} from Section 5. Each margin component is

$$\hat{m}_{j,i^*} = \hat{y}_{i^*} - \hat{y}_j = (W_{L,i^*} - W_{L,j}) \cdot \hat{z}_{L-1} + (b_{L,i^*} - b_{L,j}),$$

where W_{L,i^*} and $W_{L,j}$ denote rows i^* and j of W_L . This is essentially a single-row computation (the difference of two rows), and we can bound its deviation using techniques analogous to Section 5's layer-wise analysis.

LEMMA 6.1 (FINAL-LAYER PAIRWISE DEVIATION). *Let \hat{z}_{L-1} satisfy $\|\hat{z}_{L-1} - z_{L-1}\|_2 \leq D_{L-1}$ and $\|z_{L-1}\|_2 \leq r_{L-1}$. Suppose the conditions of Theorem 4.2 hold at layer L . Then*

$$|\hat{m}_{j,i^*} - m_{j,i^*}| \leq \alpha_L^{(j,i^*)} \cdot D_{L-1} + \beta_L^{(j,i^*)}(r_{L-1}),$$

where

$$\begin{aligned} \alpha_L^{(j,i^*)} &:= \|W_{L,i^*} - W_{L,j}\|_2 + \kappa_{nL} \cdot (\|W_{L,i^*}\| + \|W_{L,j}\|)_2, \\ \beta_L^{(j,i^*)}(r) &:= \kappa_{nL} \cdot (\|W_{L,i^*}\| + \|W_{L,j}\|)_2 \cdot r \\ &\quad + u \cdot (|b_{L,i^*}| + |b_{L,j}|) + 2(1+u) \cdot a_{\text{dot}}(nL). \end{aligned}$$

Two FP executions, two error bounds. The certification condition necessarily involves comparing two network executions: at the center x , where we observe the floating-point margin $\hat{m}_{j,i^*}(x)$ and check if it is sufficiently large; and at arbitrary $x' \in B(x, \varepsilon)$, where we must guarantee $\hat{m}_{j,i^*}(x') > 0$. Each execution incurs floating-point rounding error. We therefore introduce two error terms, E_{ctr} and E_{ball} , to bound the floating-point deviation in the margin at each point x and x' respectively. The deviation bound at a point depends on the maximum radius at which the network operates. To distinguish the two evaluations, we make the center x and perturbation radius ε explicit in the notation for r_ℓ and D_ℓ (which were left implicit in Sections 4 and 5), writing e.g., $r_\ell(x, \varepsilon)$ and $D_\ell(x, \varepsilon)$:

- At x : The input is exactly x (distance 0 from center), so we use $r_0 = \|x\|_2$ as the initial radius. Propagating this through the layer-wise recurrences from Sections 4 and 5 yields the deviation bound $D_{\text{ctr}} := D_{L-1}(x, 0)$ at layer $L-1$ and the radius bound $r_{\text{ctr}} := r_{L-1}(x, 0)$. Applying Theorem 6.1 then gives the tighter error bound

$$E_{\text{ctr}} := \alpha_L^{(j,i^*)} \cdot D_{\text{ctr}} + \beta_L^{(j,i^*)}(r_{\text{ctr}}).$$

- At $x' \in B(x, \varepsilon)$: The input can be up to ε away from x , so we use $r_0 = \|x\|_2 + \varepsilon$ as the initial radius to cover the entire ball. This yields $D_{\text{ball}} := D_{L-1}(x, \varepsilon)$ and $r_{\text{ball}} := r_{L-1}(x, \varepsilon)$, giving the looser bound

$$E_{\text{ball}} := \alpha_L^{(j, i^*)} \cdot D_{\text{ball}} + \beta_L^{(j, i^*)}(r_{\text{ball}}).$$

THEOREM 6.2 (FLOATING-POINT ROBUSTNESS CERTIFICATE). *Let $x \in \mathbb{R}^{n_1}$, $\varepsilon > 0$, and $i^* = \text{ArgMax}(N(x))$. Recall that all activations are assumed to be FP-exact (Section 3.1, assumption (iv)). Assume further that the final layer uses identity activation. Suppose:*

- (i) *The conditions of Theorem 4.2 hold at every layer with $r_0 = \|x\|_2 + \varepsilon$ (ensuring overflow-freedom over $B(x, \varepsilon)$).*
- (ii) *For each competing class $j \neq i^*$, there exists a margin Lipschitz constant $L_{j, i^*} \geq 0$ such that for all $x_1, x_2 \in \mathbb{R}^{n_1}$,*

$$|m_{j, i^*}(x_1) - m_{j, i^*}(x_2)| \leq L_{j, i^*} \cdot \|x_1 - x_2\|_2.$$

- (iii) *The certification condition holds for each $j \neq i^*$, where E_{ctr} and E_{ball} are the error bounds defined above for the pair (i^*, j) :*

$$\hat{m}_{j, i^*}(x) - L_{j, i^*} \cdot \varepsilon - (E_{\text{ctr}} + E_{\text{ball}}) > 0.$$

Then for all $x' \in B(x, \varepsilon)$ at which the floating-point network executes without overflow (which is guaranteed by assumption (i)), the floating-point margin $\hat{m}_{j, i^}(x') > 0$ for every $j \neq i^*$, and hence $\text{ArgMax}(\hat{N}(x')) = \text{ArgMax}(\hat{N}(x)) = i^*$ (classification is preserved under floating-point execution).*

Connection to classical certification. The classical real arithmetic margin certification approach (Section 2.1) requires $m_{j, i^*}(x) > L_{j, i^*} \cdot \varepsilon$ for each competing class j . Thus the additional term $(E_{\text{ctr}} + E_{\text{ball}})$ quantifies the *margin degradation* due to floating-point errors. This degradation is instance-dependent, varying with both the input point and perturbation radius, as well as the floating-point format and network complexity. Generally speaking, the margin degradation is much smaller for higher-precision formats, and worse for lower-precision ones; Section 8 quantifies the margin degradation for practical models.

7 Pre-Deployment Hybrid Certification

The deviation bounds D_ℓ of Section 6 are worst-case bounds. They are designed to be efficiently computable from the network properties and (worst-case) deviation D_ℓ of Section 5. As we will see later in Section 8, this necessarily means that for larger-scale networks they can be very conservative, which hampers the precision (though not soundness) of robustness certification.

In this section, we explore how these bounds can be made tighter in a *pre-deployment* setting, in which robustness certification is being used to evaluate a model before it is deployed. This is the setting in which robustness verifiers [22] are often applicable. Many such verifiers are orders of magnitude slower than robustness certifiers and so are more difficult to apply to evaluate model outputs at deployment-time, at which answers are needed in milliseconds. The pre-deployment setting is therefore an important use-case for robustness checkers.

Our key idea is that quantities like D_ℓ can be very conservative at lower-precision formats; however, are very tight at high-precision formats like float64. Also, while one's goal might be to evaluate the robustness of a model executing in a standard format like float32, at pre-deployment time it is possible to take measurements from a high-precision execution of the model (e.g., float64) and to combine those with tight high-precision format deviation bounds to much more tightly bound deviation than the worst-case quantity D_ℓ .

Specifically, for the deviation bound at the penultimate layer $L - 1$, given an input point x one can measure the actual deviation between the target model (e.g., executing in float32) and a

higher-precision execution of the same model on the same input (e.g., at float64). This measured deviation will be incredibly close to the deviation between the target model and real arithmetic, and indeed we can close the tiny gap between the high-precision execution and real arithmetic by simply adding on the worst-case deviation for the high-precision model. Using the superscript hi to denote the high-precision execution, we therefore define the *hybrid* deviation for an input point x as follows:

$$D_{L-1}^{\text{hybrid}}(x) := \|\hat{z}_{L-1}(x) - \hat{z}_{L-1}^{\text{hi}}(x)\|_2 + D_{L-1}^{\text{hi}}(x, 0)$$

Since $\|d_{L-1}^{\text{hi}}\|_2 \leq D_{L-1}^{\text{hi}}$ by Theorem 5.2 and via the triangle inequality we have the following:

LEMMA 7.1 (HYBRID DEVIATION BOUND.). *For an input point x :*

$$\|d_{L-1}(x)\|_2 \leq D_{L-1}^{\text{hybrid}}(x)$$

Moreover, this means we can instantiate Theorem 6.1 for the single input point x and $\varepsilon = 0$ with $D_{L-1}^{\text{hybrid}}(x)$ in place of D_{L-1} . As a result, we can use $D_{L-1}^{\text{hybrid}}(x)$ in place of D_{ctr} when computing E_{ctr} when performing the certification check of Theorem 6.2, i.e., E_{ctr} can be soundly replaced by:

$$E_{\text{ctr}}^{\text{hybrid}} := \alpha_L^{(j,i^*)} \cdot D_{L-1}^{\text{hybrid}}(x) + \beta_L^{(j,i^*)}(r_{\text{ctr}}).$$

THEOREM 7.2. *Let the conditions of Theorem 6.2 hold for an input point x , except the certification check is replaced by:*

$$\hat{m}_{j,i^*}(x) - L_{j,i^*} \cdot \varepsilon - (E_{\text{ctr}}^{\text{hybrid}} + E_{\text{ball}}) > 0.$$

Then, as in Theorem 6.2, x is robust for ε .

In practice, this replacement significantly reduces the size of E_{ctr} and leads to more precise robustness certification, at the expense of having to run model forward passes at high precision.

Note: the same trick cannot be used for E_{ball} since it captures the error for the arbitrary $x' \in B(x, \varepsilon)$, rather than for the centre input point x for which we can directly bound x' 's deviation using the high-precision execution. For the same reason, overflow checking (Section 4) must still use the conservative quantities.

8 Evaluation

We structure the evaluation around three research questions. **RQ1** asks whether floating-point-aware certification correctly avoids the false certificates identified in Section 2.3. **RQ2** assesses whether it is fast and precise enough for practical use on standard benchmarks. **RQ3** compares the hybrid pre-deployment method (Section 7) against ERAN [35], the only publicly available pre-deployment robustness verifier of which we are aware that is sound with respect to the floating-point semantics of neural networks.

8.1 Experimental Setup

Implementation. We implemented the certification procedure in approximately 2,000 source lines of Python code. The implementation extends a re-implementation of Tobler et al.'s classical real arithmetic certifier [42] (which we validate against their reference outputs) with floating-point-aware components for overflow analysis (Section 4), deviation bounding (Section 5), margin certification (Section 6), and the hybrid pre-deployment certification optimisation (Section 7). The floating-point extensions are almost double the size of the classical certification kernel, reflecting the non-trivial additional reasoning required to soundly account for rounding errors. As with Tobler et al.'s certifier [42] all bound computations use arbitrary-precision rational arithmetic via the gmpy2 library to avoid introducing floating-point errors in the certifier itself.

Models and datasets. We evaluate on three globally robust neural network classifiers trained by Tobler et al. [42]:

- **MNIST** [29]: 8 hidden layers of 128 neurons each
- **Fashion MNIST** [49]: 12 hidden layers (first layer: 256 neurons, remaining 11 layers: 128 neurons each)
- **CIFAR-10** [27]: 8 hidden layers (512, 256, then 6 layers of 128 neurons each)

All models use only fully-connected (i.e. dense) layers with ReLU activations on hidden layers, identity activation on the output layer, and float32 weights and activations in deployment. Input and output dimensions are standard for the respective datasets (784 and 10 for both MNIST and Fashion MNIST; 3072 and 10 for CIFAR-10). See [42, Table 1] for complete architectural details and [43, Appendix E] for model training hyperparameters.

Our experiments use pre-computed weight matrix norms: $\|W_\ell\|_2$ and $\|W_\ell\|_2$, which are computed using the same (RQ2 and RQ3) or higher (RQ1) number of Gram iterations as in [42, Table 1]; for RQ2 and RQ3 all $\|W_\ell\|_2$ are identical to those computed by Tobler et al.’s verified certifier [42].

We evaluate on two types of instances:

- **Standard test sets:** The complete standard evaluation benchmarks for each classification task (10,000 test instances per dataset), representing the full test distribution
- **Counterexample instances:** Adversarially-crafted instances (see Section 2.3) that expose the semantic gap in real arithmetic certification

Floating-point formats. We consider float16, float32, and float64 execution semantics, with float32 as the primary focus: it is the standard deployment format for the models we evaluate and the format in which the models were trained [42]. As discussed in Section 4, the practical requirement $n_\ell \cdot u \ll 1$ excludes bfloat16 altogether from evaluation. For float16, while overflow certification succeeds, robustness certification is vacuous: the conservatism is so severe that no instances from the standard test sets are certified as robust, even with the hybrid optimisation (Section 7). The main results (RQ2 and RQ3) therefore focus on float32; all three formats are included in RQ1.

8.2 Soundness: Closing the Semantic Gap

8.2.1 RQ1: Does floating-point-aware certification avoid false certificates? As described in Section 2.3, real arithmetic certifiers produce misleading robustness certificates for instances positioned near floating-point-induced decision boundaries. We test whether our floating-point-aware certifier correctly rejects counterexample instances generated using the procedure described in Section 2.3, across all three models and all three floating-point formats (float16, float32, float64), except CIFAR-10 at float16 since in this configuration the practical constraint $n_\ell \cdot u < 1$ is violated (Section 4), generating at least 30 adversarial instances per combination. When running these tests we use an increased number of Gram iterations when computing the matrix norms used during certification compared to Tobler et al. [42], which leads to tighter norm bounds and therefore less conservative certifications, for MNIST and Fashion MNIST. Specifically, we use 20 Gram iterations for MNIST, 13 for Fashion MNIST, and 12 for CIFAR-10 (compared to 11, 12, and 12 respectively in Tobler et al. [42] and all subsequent experiments reported in this paper).

Finding. In all cases, real arithmetic certifiers (including Tobler et al. [42]) would certify these instances as robust, despite their actual vulnerability under floating-point execution. Our floating-point-aware certifier correctly rejected *all* of them across all eight model-format combinations (0% certified), and even under the tighter pre-deployment hybrid certification check (Section 7), confirming that the theory successfully closes the semantic gap. By accounting for floating-point

rounding throughout the network, we avoid producing false robustness guarantees for instances specifically crafted to expose the discrepancy between real and floating-point arithmetic.

8.3 Practicality and Coverage

8.3.1 RQ2: Is certification practical on standard benchmarks? We now evaluate on the complete standard test sets for each classification task to assess performance and coverage on the full test distribution (as opposed to the adversarial counterexamples above).

Dataset	ϵ	Per-Instance Time (Avg)	Verified Robustness (Real)	Verified Robustness (FP)	Δ Robustness	Margin Increase
MNIST	0.3	0.78ms	95.74%	95.50%	0.24	4%
Fashion MNIST	0.25	1.00ms	83.65%	82.16%	1.49	9%
CIFAR-10	0.141	1.38ms	46.12%	18.90%	27.22	109%

Table 1. Float32 certification results on standard test sets (10,000 points per model). Perturbation radii (ϵ) follow Tobler et al. [42]. Time measurements use pre-computed weight norms. “Verified Robustness (Real)” shows percentage certified under real arithmetic assumptions (and are identical to Tobler et al. [42]). “Verified Robustness (FP)” shows percentage certified under floating-point execution. “ Δ Robustness” is the difference in percentage points between the two. “Margin Increase” shows the average relative increase in certification margin required to account for floating-point errors.

Finding. Certification is practical and the theory is non-vacuous. Certification is fast (0.78–1.38ms per instance) and maintains substantial coverage (Table 1). Even accounting for floating-point effects, we certify 95.5% of MNIST instances, 82.2% of Fashion MNIST instances, and 18.9% of CIFAR-10 instances as robust at their respective perturbation radii. The gap between real and floating-point certification rates is small for MNIST (0.24 pp) and Fashion MNIST (1.49 pp) but substantial for CIFAR-10 (27.22 pp), where the larger input dimension drives greater error accumulation—reflected in the 109% average margin increase required for that model.

8.3.2 RQ3: Pre-Deployment Certification: Coverage and Competitiveness. The problem that our pre-deployment certification method (Section 7) solves is how to certify the robustness of a model over a distribution, such as its standard test distribution. In this setting, the quantity of interest is the model’s Verified Robust Accuracy (VRA): the proportion of points that it correctly classifies and that are certified or verified to be robust. There are two questions of interest here: first, how much does FP-aware certification degrade VRA relative to a real arithmetic certifier? Second, how does our method compare to ERAN [35], which is—to our knowledge—the only publicly available robustness verifier that claims soundness against the floating-point execution semantics of neural networks and that has been applied to compute VRA statistics for models on the scale of those used in our evaluation.

Setup. ERAN operates on ℓ_∞ -robustness rather than the ℓ_2 -robustness of our approach. We convert our ϵ_{ℓ_2} values to a comparable ℓ_∞ radius via

$$\epsilon_{\ell_\infty} \approx \epsilon_{\ell_2} / \sqrt{n_{\text{in}}},$$

where n_{in} is the input dimension (784 for MNIST and Fashion MNIST; 3072 for CIFAR-10). Importantly, the ℓ_∞ ball of radius $\varepsilon_{\ell_\infty}$ is *contained within* our ℓ_2 ball of radius ε_{ℓ_2} : ERAN therefore certifies against a strictly smaller set of perturbations, making its task easier and its guarantee weaker.

Following the evaluation protocol of [38, 39], we run ERAN using the DeepPoly abstract domain [39] on 100 instances (test points) per model. ERAN requires tens of seconds to verify each instance [39]. Our prototype runs in milliseconds per instance, enabling evaluation over all 10,000 standard test points.

Dataset	Perturbation Radius		Verified Robust Accuracy (VRA)		
	ε_{ℓ_2} (Ours)	$\varepsilon_{\ell_\infty}$ (ERAN)	Real (Ours)	FP (Ours)	ERAN
MNIST	0.3	0.011	95.40%	95.27%	99%
Fashion MNIST	0.25	0.00893	79.54%	78.94%	53%
CIFAR-10	0.141	0.0025	35.95%	25.57%	47%

Table 2. Float32 hybrid certification results (10,000 points per model) compared to ERAN (100 points per model, DeepPoly abstract domain [39]). ERAN $\varepsilon_{\ell_\infty}$ values are derived from ours via $\varepsilon_{\ell_\infty} \approx \varepsilon_{\ell_2} / \sqrt{n_{\text{in}}}$. “Real (Ours)” shows VRA under real arithmetic assumptions (from Tobler et al. [42]); “FP (Ours)” shows VRA under floating-point execution using the hybrid pre-deployment method (Section 7).

Finding (FP overhead). The increased conservatism of FP-aware pre-deployment certification is small for MNIST and Fashion MNIST but more significant for CIFAR-10 (~10 percentage points), consistent with the pattern seen in **RQ2**: larger input dimensions lead to greater error accumulation. However, we note that the degradation is significantly lower when using the pre-deployment certification method.

Finding (ERAN comparison). Despite certifying a *stronger* property than ERAN, our method achieves comparable or superior VRA on two of the three benchmarks (Table 2). On MNIST the result is within 4 percentage points: almost certainly within the sampling error inherent in the ERAN results (which compute VRA over a sample of 100 out of 10,000 test points). On Fashion MNIST we substantially outperform ERAN by more than 15 percentage points. For CIFAR-10, our analysis is considerably more conservative than ERAN’s, which achieves much higher VRA than even the classical real arithmetic Lipschitz-based certifier. This is perhaps not surprising given that ERAN is verifying a weaker guarantee. Accounting for floating-point rounding, even with the hybrid optimisation applied, adds non-trivial conservatism for the CIFAR-10 model.

8.4 Discussion

Overall our results are positive, while clarifying the practical cost of ensuring soundness against floating-point execution semantics rather than real arithmetic abstractions.

The experiments highlight a fundamental precision-dependent limitation. For float16, robustness certification becomes vacuous on standard benchmarks, although absence of overflow can be certified. This suggests that precise floating-point-sound certification is intrinsically more challenging at low precision, even though (as the results of Section 2.3 demonstrate) it is precisely at low precision that floating-point rounding becomes most dangerous for soundly certifying robustness. Guarantees for aggressively quantised deployment may require tighter deviation bounds or alternative reasoning techniques.

9 Related Work

This paper tackles the problem of how to soundly account for floating-point rounding in machine learning models when doing Lipschitz sensitivity-based robustness certification.

We motivated our investigation by constructing adversarial inputs that are misleadingly certified robust (often at very small ε) by Lipschitz-based certifiers, despite the existence of counterexample points within ε that the model classifies differently due to floating-point rounding. Jia and Ri-nard [19] first demonstrated a similar phenomenon for complete robustness verifiers, at much larger, semantically meaningful values of ε . Subsequent work also showed how to construct backdoored networks together with specific trigger inputs for which a complete verifier claims robustness under its arithmetic model, yet counterexamples exist under floating-point execution [54]. More recently, Szász et al. [41] go further and show how low-level details like the order of operations, mixed-precision implementations, and other specifics of the execution runtime, can lead to robustness verifiers giving misleading results for specially crafted networks. Our theory does not explicitly handle such details, if they depart from standard floating-point semantics. We return to this point in Section 10.

The problem of how to account for floating-point rounding in program implementations when reasoning about them has been well studied [11, 17] since at least the late 1950s and the seminal work of Wilkinson [47]. This paper is built upon the well-studied wealth of results bounding floating-point error in linear algebra programs and our Rocq formalisation is built on top of the LAProof library [23] which formalises the key results from this area.

We are not the first to apply classical floating-point error analysis to neural networks. Very recently, Beuzeville et al. [6] developed a framework providing both deterministic and probabilistic bounds. Most closely related to our work is their deterministic theorem [6, Theorem 2], which establishes a classical componentwise backward-error result for feed-forward networks: the computed output is shown to coincide with the exact output of a network with slightly perturbed parameters, with perturbations controlled by the classical floating-point relative-error model for arithmetic operations [17] (implicitly assuming results remain normalised) and extended to account for activation rounding via condition-number bounds. In contrast, our most closely-related result (Theorem 5.2) derives a forward, normwise deviation bound. We explicitly decompose rounding effects into amplification of prior deviation and fresh per-layer error contributions, yielding a linear recursion for the ℓ_2 -norm of the deviation. Crucially, this bound holds uniformly for all inputs in the ε -ball, enabling its direct use in robustness certification. Our analysis also explicitly treats both overflow and gradual underflow, interleaving overflow-freedom certification with deviation propagation; these aspects are not addressed in Beuzeville et al. Finally, while our analysis assumes floating-point exact entrywise activations (e.g., ReLU), Beuzeville et al. treat differentiable activations and explicitly account for their rounding error. Their treatment of activation rounding could potentially be incorporated to extend our framework to a broader class of activation functions.

Closely related in spirit, El Arar et al. [2] develop a classical forward error analysis for feed-forward neural network inference and use it to guide mixed-precision accumulation strategies, in which one selectively recomputes numerically sensitive inner products in higher precision to improve cost-accuracy trade-offs. Similar to Beuzeville et al. [6], their analysis propagates floating-point rounding error through the network layer by layer under the standard relative-error model and assumes absence of overflow and underflow. However, their goal is performance optimisation rather than certification: the resulting bounds are componentwise and input-specific, and are used to identify sensitive computations rather than to certify robustness uniformly over an ε -ball.

Lipschitz-based robustness certification rose to prominence with the work of Leino et al. [30], which has since been extended to cover large (billion-parameter) models with impressive precision [18]. Until now, the problem of how Lipschitz-based robustness certification should account for floating-point rounding in neural network execution has remained unaddressed.

Certified robustness checking is but one way to obtain robustness guarantees for neural networks, by performing numeric computation (such as Lipschitz constants) used during certification. Another prominent line of work focuses on applying formal verification or symbolic reasoning over the neural network itself to check for input robustness. A large array of verification tools have been produced and now annually compete to solve yet more challenging verification tasks [22]. Almost none of these tools account for floating-point rounding in the neural networks that they verify.

Almost all of these tools focus on verification problems involving individual inputs, rather than producing distribution-level guarantees as is common for certified robustness mechanisms, such as Verified Robust Accuracy (VRA) which was the quantity of interest for our pre-deployment certification scenario studied in Section 8.3.2.

Verifiers such as PyRAT [31] ensure that the floating-point computations performed within the verifier do not compromise soundness with respect to a real arithmetic semantics of neural networks. However, their formal guarantees are stated relative to real semantics, rather than to the floating-point execution semantics, of the neural network itself. Other verifiers like α, β -CROWN [37, 45, 50, 51, 53], Marabou [21, 48], NeuralSAT [12–14], nenum [3, 4], CORA [1, 24–26, 28], NeVer2 [9, 16], and NNV [32, 44] avoid claiming soundness with respect to the neural network’s floating-point implementation or focus on proving properties of single inputs (e.g. expressed in VNN-LIB [10]); rather than distribution-level guarantees.

Some verifiers were specifically designed to be sound under floating-point neural network semantics. Prominent examples are the abstract interpretation-based DeepZ [38] and the more recent DeepPoly [39], embodied in the ERAN tool [35] against which we compared in Section 8. The more recent FMIPVerify [52] applies Mixed Integer Linear Programming (MILP) to soundly reason about floating-point neural networks via an abstraction to real-number interval arithmetic; however, they evaluate only on downsampled (7×7) MNIST and Fashion MNIST models that are about an order of magnitude smaller than those on which we evaluate in Section 8.

Another strand of floating-point sound neural network verification research applies floating-point sound program verifiers to reason about neural networks by first translating them into programs in common programming languages like C. Examples include QNNVerifier [40] as well as [33]. However, these methods necessarily face severe scalability challenges, because they tend to employ very precise reasoning methods like SMT solving or software model checking. As a result, they focus on properties of individual inputs rather than distribution-level guarantees.

10 Conclusion

In this paper we identify how Lipschitz-based robustness certification can be semantically unsound under float-point neural network execution. To do so we showed concrete counterexamples that cause even a formally verified certifier to give misleading answers. Focusing on feed-forward networks with ReLU activations, we showed how to certify the absence of overflow and constructed a compositional bound on the deviation between floating-point and real arithmetic execution, which can be operationalised through interleaved application layer-by-layer through a neural network. We showed how this bound can be applied by modifying the classical real arithmetic certification condition to account for floating-point rounding. This yields a quantification on the degradation of the robustness certificate under floating-point execution. We showed how this degradation can be halved when certification is performed pre-deployment, by taking advantage of deviation measurements from a high-precision (e.g., float64) execution. We mechanised our theory in the

Rocq theorem prover, and implemented it within a Python based certifier. We empirically evaluated our certifier, demonstrating that our methods are practical for MNIST and CIFAR-10 scale networks.

Many of our results in this paper are specialised to fully-connected ReLU networks with identity output activation, as in [42]. Extending floating-point aware certification to networks involving convolutional layers, batch normalization, residual connections, and other architectural features common in modern classifiers is a natural direction for future work.

Our analysis assumes IEEE-style floating-point semantics with round-to-nearest and gradual underflow (i.e., subnormals). Real-world deployments may instead employ fused operators, hardware-specific kernels, flush-to-zero (FTZ) semantics, or reduced-precision accelerators whose operational semantics deviate from this model. Recent work has shown how such low-level execution details can undermine the guarantees of robustness verifiers that are sound with respect to a floating-point execution semantics, when the deployed runtime does not conform to the semantics assumed by the verifier [41]. Extending our theory to encompass alternative or hardware-specific floating-point behaviours is a natural direction for future work.

References

- [1] Althoff, M.: An introduction to CORA 2015. In: Proc. of the Workshop on Applied Verification for Continuous and Hybrid Systems (ARCH). pp. 120–151 (2015)
- [2] Arar, E.M.E., Filip, S.I., Mary, T., Riccietti, E.: Mixed precision accumulation for neural network inference guided by componentwise forward error analysis. *IMA Journal of Numerical Analysis* **1**, 21 (2025)
- [3] Bak, S.: nnenum: Verification of ReLU neural networks with optimized abstraction refinement. In: NASA Formal Methods Symposium. pp. 19–36. Springer (2021)
- [4] Bak, S., Tran, H.D., Hobbs, K., Johnson, T.T.: Improved geometric path enumeration for verifying ReLU neural networks. In: 32nd International Conference on Computer-Aided Verification (CAV) (July 2020)
- [5] Bertot, Y., Castéran, P.: Interactive theorem proving and program development: Coq’Art: the calculus of inductive constructions. Springer Science & Business Media (2013)
- [6] Beuzeville, T., Buttari, A., Gratton, S., Mary, T.: Deterministic and probabilistic rounding error analysis of neural networks in floating-point arithmetic. *IMA Journal of Numerical Analysis* p. draft30 (2026)
- [7] Cordeiro, L.C., Daggitt, M.L., Girard-Satabin, J., Isac, O., Johnson, T.T., Katz, G., Komendantskaya, E., Lemesle, A., Manino, E., Šinkarovs, A., et al.: Neural network verification is a programming language challenge. In: European Symposium on Programming. pp. 206–235. Springer (2025)
- [8] Delattre, B., Barthélemy, Q., Araujo, A., Allauzen, A.: Efficient bound of Lipschitz constant for convolutional layers by Gram iteration. In: International Conference on Machine Learning (ICML). pp. 7513–7532. PMLR (2023)
- [9] Demarchi, S., Guidotti, D., Pulina, L., Tacchella, A.: NeVer2: Learning and verification of neural networks. *Soft Computing* (2024)
- [10] Demarchi, S., Guidotti, D., Pulina, L., Tacchella, A., Narodytska, N., Amir, G., Katz, G., Isac, O.: Supporting standardization of neural networks verification with VNN-LIB and CoCoNet. In: FoMLAS. pp. 47–58 (2023)
- [11] Demmel, J.W.: Applied numerical linear algebra. SIAM (1997)
- [12] Duong, H., Li, L., Nguyen, T., Dwyer, M.: A DPLL(T) framework for verifying deep neural networks (2023), arXiv, 25 pages
- [13] Duong, H., Nguyen, T., Dwyer, M.B.: NeuralSAT: A high-performance verification tool for deep neural networks. In: International Conference on Computer Aided Verification. pp. 409–423. Springer (2025)
- [14] Duong, H., Xu, D., Nguyen, T., Dwyer, M.B.: Harnessing neuron stability to improve DNN verification. *Proceedings of the ACM on Software Engineering* **1**(FSE), 859–881 (2024)
- [15] Gouk, H., Frank, E., Pfahringer, B., Cree, M.J.: Regularisation of neural networks by enforcing Lipschitz continuity. *Mach. Learn.* **110**(2), 393–416 (2021). <https://doi.org/10.1007/S10994-020-05929-W>, <https://doi.org/10.1007/s10994-020-05929-w>
- [16] Guidotti, D., Pulina, L., Tacchella, A.: pyNeVer: A framework for learning and verification of neural networks. In: Automated Technology for Verification and Analysis: 19th International Symposium, ATVA 2021, Gold Coast, QL D, Australia, October 18–22, 2021, Proceedings 19. pp. 357–363. Springer (2021)
- [17] Higham, N.J.: Accuracy and stability of numerical algorithms. SIAM (2002)
- [18] Hu, K., Hu, H., Fredrikson, M.: Lipnext: Scaling up lipschitz-based certified robustness to billion-parameter models. arXiv preprint arXiv:2601.18513 (2026)

- [19] Jia, K., Rinard, M.: Exploiting verified neural networks via floating point numerical error. In: International Static Analysis Symposium. pp. 191–205. Springer (2021)
- [20] Katz, G., Barrett, C., Dill, D.L., Julian, K., Kochenderfer, M.J.: Reluplex: An efficient SMT solver for verifying deep neural networks. In: International Conference on Computer Aided Verification (CAV). pp. 97–117. Springer (2017)
- [21] Katz, G., Huang, D.A., Ibeling, D., Julian, K., Lazarus, C., Lim, R., Shah, P., Thakoor, S., Wu, H., Zeljić, A., et al.: The Marabou> framework for verification and analysis of deep neural networks. In: International Conference on Computer Aided Verification. pp. 443–452. Springer (2019)
- [22] Kaulen, K., Ladner, T., Bak, S., Brix, C., Duong, H., Flinkow, T., Johnson, T.T., Koller, L., Manino, E., Nguyen, T.H., et al.: The 6th international verification of neural networks competition (VNN-COMP 2025): Summary and results. arXiv preprint arXiv:2512.19007 (2025)
- [23] Kellison, A.E., Appel, A.W., Tekriwal, M., Bindel, D.: LAPProof: A library of formal proofs of accuracy and correctness for linear algebra programs. In: 2023 IEEE 30th Symposium on Computer Arithmetic (ARITH). pp. 36–43. IEEE (2023)
- [24] Kochdumper, N., Schilling, C., Althoff, M., Bak, S.: Open- and closed-loop neural network verification using polynomial zonotopes. In: NASA Formal Methods. pp. 16–36 (2023)
- [25] Koller, L., Ladner, T., Althoff, M.: Out of the shadows: Exploring a latent space for neural network verification. arXiv (2025)
- [26] Koller, L., Ladner, T., Althoff, M.: Set-based training for neural network verification. TMLR (2025)
- [27] Krizhevsky, A.: Learning multiple layers of features from tiny images. Tech. rep., University of Toronto (2009)
- [28] Ladner, T., Althoff, M.: Automatic abstraction refinement in neural network verification using sensitivity analysis. In: Proc. of the Int. Conf. on Hybrid Systems: Computation and Control (HSCC). pp. 1–13 (2023)
- [29] LeCun, Y., Bottou, L., Bengio, Y., Haffner, P.: Gradient-based learning applied to document recognition. Proceedings of the IEEE **86**(11), 2278–2324 (1998)
- [30] Leino, K., Wang, Z., Fredrikson, M.: Globally-robust neural networks. In: International Conference on Machine Learning (ICML). Proceedings of Machine Learning Research, vol. 139, pp. 6212–6222. PMLR (2021), <http://proceedings.mlr.press/v139/leino21a.html>
- [31] Lemesle, A., Lehmann, J., Tristan, L.G.: Neural network verification with PyRAT. arXiv preprint arXiv:2410.23903 (2024)
- [32] Lopez, D.M., Choi, S.W., Tran, H.D., Johnson, T.T.: NNV 2.0: The neural network verification tool. In: 35th International Conference on Computer-Aided Verification (CAV) (July 2023)
- [33] Manino, E., Farias, B., Menezes, R.S., Shmarov, F., Cordeiro, L.C.: Floating-point neural network verification at the software level. arXiv preprint arXiv:2510.23389 (2025)
- [34] Moosavi-Dezfooli, S.M., Fawzi, A., Frossard, P.: Deepfool: a simple and accurate method to fool deep neural networks (2015)
- [35] Müller, M.N., Singh, G., Balunovic, M., Makarchuk, G., Ruoss, A., Serre, F., Baader, M., Drachler-Cohen, D., Gehr, T., Hoffmann, A., Maurer, J., Müller, C., Püschel, M., Tsankov, P., Vechev, M.: ERAN: ETH robustness analyzer for neural networks. <https://github.com/eth-sri/eran> (2018), secure, Reliable, and Intelligent Systems Lab, ETH Zürich
- [36] Nicolae, M.I., Sinn, M., Tran, M.N., Buesser, B., Rawat, A., Wistuba, M., Zantedeschi, V., Baracaldo, N., Chen, B., Ludwig, H., et al.: Adversarial Robustness Toolbox v1.0.0. arXiv preprint arXiv:1807.01069 (2018)
- [37] Shi, Z., Jin, Q., Kolter, Z., Jana, S., Hsieh, C.J., Zhang, H.: Neural network verification with branch-and-bound for general nonlinearities. arXiv preprint arXiv:2405.21063 (2024)
- [38] Singh, G., Gehr, T., Mirman, M., Püschel, M., Vechev, M.: Fast and effective robustness certification. Advances in neural information processing systems **31** (2018)
- [39] Singh, G., Gehr, T., Püschel, M., Vechev, M.: An abstract domain for certifying neural networks. Proceedings of the ACM on Programming Languages **3**(POPL), 1–30 (2019)
- [40] Song, X., Manino, E., Sena, L., Alves, E., Bessa, I., Lujan, M., Cordeiro, L., et al.: QNNVerifier: A tool for verifying neural networks using SMT-based model checking. arXiv preprint arXiv:2111.13110 (2021)
- [41] Szász, A., Bánhelyi, B., Jelasity, M.: No soundness in the real world: On the challenges of the verification of deployed neural networks. arXiv preprint arXiv:2506.01054 (2025)
- [42] Tobler, J., Syeda, H.T., Murray, T.: A formally verified robustness certifier for neural networks. In: International Conference on Computer Aided Verification (CAV). pp. 327–348. Springer (2025)
- [43] Tobler, J., Syeda, H.T., Murray, T.: A formally verified robustness certifier for neural networks (extended version) (2025), <https://arxiv.org/abs/2505.06958>
- [44] Tran, H.D., Yang, X., Lopez, D.M., Musau, P., Nguyen, L.V., Xiang, W., Bak, S., Johnson, T.T.: NNV: The neural network verification tool for deep neural networks and learning-enabled cyber-physical system s. In: 32nd International Conference on Computer-Aided Verification (CAV) (July 2020)
- [45] Wang, S., Zhang, H., Xu, K., Lin, X., Jana, S., Hsieh, C.J., Kolter, Z.: Beta-CROWN: Efficient bound propagation with per-neuron split constraints for complete and incomplete neural network verification. arXiv preprint arXiv:2103.06624

- (2021)
- [46] Weng, L., Zhang, H., Chen, H., Song, Z., Hsieh, C.J., Daniel, L., Boning, D., Dhillon, I.: Towards fast computation of certified robustness for relu networks. In: International Conference on Machine Learning (ICML). pp. 5276–5285. PMLR (2018)
 - [47] Wilkinson, J.H.: Error analysis of floating-point computation. *Numerische Mathematik* **2**(1), 319–340 (1960)
 - [48] Wu, H., Isac, O., Zeljić, A., Tagomori, T., Daggitt, M., Kokke, W., Refaeli, I., Amir, G., Julian, K., Bassan, S., et al.: Marabou 2.0: a versatile formal analyzer of neural networks. In: International Conference on Computer Aided Verification. pp. 249–264. Springer (2024)
 - [49] Xiao, H., Rasul, K., Vollgraf, R.: Fashion-MNIST: a novel image dataset for benchmarking machine learning algorithms. arXiv preprint arXiv:1708.07747 (2017)
 - [50] Xu, K., Shi, Z., Zhang, H., Wang, Y., Chang, K.W., Huang, M., Kailkhura, B., Lin, X., Hsieh, C.J.: Automatic perturbation analysis for scalable certified robustness and beyond. *Advances in Neural Information Processing Systems* **33** (2020)
 - [51] Xu, K., Zhang, H., Wang, S., Wang, Y., Jana, S., Lin, X., Hsieh, C.J.: Fast and Complete: Enabling complete neural network verification with rapid and massively parallel incomplete verifiers. In: International Conference on Learning Representations (2021), <https://openreview.net/forum?id=nVZtXB16LNn>
 - [52] Yang, S., Chen, L., Yin, B., Li, M., Zhou, Y., Wang, J.: Sound floating-point neural network verification with MILP. In: Asia-Pacific Software Engineering Conference (APSEC). pp. 01–10. IEEE (2024)
 - [53] Zhang, H., Wang, S., Xu, K., Li, L., Li, B., Jana, S., Hsieh, C.J., Kolter, J.Z.: General cutting planes for bound-propagation-based neural network verification. *Advances in Neural Information Processing Systems (NeurIPS)* (2022)
 - [54] Zombori, D., Bánhelyi, B., Csendes, T., Megyeri, I., Jelasity, M.: Fooling a complete neural network verifier. In: International Conference on Learning Representations (2021)